

Enhanced Amount and Quality of Alginate-like Exopolysaccharides in Aerobic Granular Sludge for the Treatment of Salty Wastewater

Fansheng Meng, Dongfang Liu, Yuwei Pan, Limeng Xi, Dan Yang, and Wenli Huang *

Osmotic pressure provided by salty wastewaters is an important influencing factor for alginate-like exopolysaccharides (ALE) in aerobic granular sludge (AGS). Therefore, research on the influence of salinity (NaCl 0 R1, 10 g/L R2, 30 g/L R3) on AGS and its ALE formation was conducted. A salinity of 1% induced larger particle size with smooth spheroidal shape and enhanced granular strength in R2. The TOC and ammonia removal were unaffected in both R2 and R3, but the P removal was greatly enhanced. ALE was much enriched at moderate salinity (1% NaCl). The amount of ALE reached 49.8 mg/g VSS at 140 d in R2, which was much higher than in R1 (26.8 mg/g VSS) and R3 (28.9 mg/g VSS), possibly due to the activation of gene *algC* expression in AGS of R2. ALE also showed the largest GG block fractionation and MW in R2, which indicated the greatest enhancement of mechanical properties. Moreover, enrichment of glucosamine, lipid content, and octadecanamide derivative in ALE of R2 endowed it with medicinal potential, stronger water-barrier property, and reduction of the products' friction coefficients, respectively. Therefore, AGS based on ALE is a potential technology for treatment of salty wastewater.

Keywords: Salty wastewater; Aerobic granular sludge; Alginate-like exopolysaccharides; P removal

Contact information: Key Laboratory of Pollution Process and Environmental Criteria, Ministry of Education; College of Environmental Science and Engineering, Nankai University, Tianjin 300350, China; *Corresponding author: huangwenli@nankai.edu.cn

INTRODUCTION

Salty wastewaters are generated from many sources, such as food, chemical, pharmaceutical, papermaking, petroleum refinery, dyeing factories, and mariculture in coastal areas (Wan *et al.* 2014; Liang *et al.* 2017; Pan *et al.* 2018). For traditional biological treatment, plasmolysis and eventual death of microorganisms are easily induced by the high osmotic pressure when the salinity is greater than 1% (Jorfi *et al.* 2017). Aerobic granular sludge (AGS) is an efficient and innovative approach for saline wastewater treatment because it has many incomparable advantages such as compact structure, good settling performance, high resistance to toxicity, and high tolerance of salinity (Wang *et al.* 2015; He *et al.* 2017; Thwaites *et al.* 2017; Morais *et al.* 2018). While some research has focused on using AGS to treat high saline wastewater (Wang *et al.* 2015; Corsino *et al.* 2017), excess sludge from AGS systems is a challenge because the cost is too high for the sludge handling (Lin *et al.* 2015). Therefore, new pathways are needed for excess AGS disposal.

Alginate is a group of linear polysaccharides that is widely used in food systems and pharmaceutical products because of its peculiar rheological properties (Peña *et al.* 2008; Borazjani *et al.* 2017). In terms of chemicals and structure, alginate macromolecules

are composed of mannuronic acid (M) and guluronic acid (G) residues. These MM and MG blocks provide the chains with flexibility, while GG blocks are generally associated with gel-forming capacity (Lin *et al.* 2010). At present, commercial alginates are mainly produced by brown algae. However, production is limited due to the restricted algae source (Díaz-Barrera *et al.* 2011). Bacteria belonging to the *Pseudomonas* and *Azotobacter* genera also produce alginate, but the cost is relatively high (Saude *et al.* 2002; Díaz-Barrera *et al.* 2011; Flores *et al.* 2013). Thus, new economic available resources for alginate extraction are needed.

Recently, alginate-like exopolysaccharides (ALE) have been extracted from aerobic granular sludge, and they possess similar characteristics as standard sodium alginate (Lin *et al.* 2010, 2013). Lin *et al.* (2013) reported that ALE exists in both aerobic granular sludge and flocculent sludge, but the amount of ALE in granular sludge was twice as much as in activated sludge (160 ± 4 mg/g VSS and 72 ± 6 mg/g VSS, respectively). Higher GG block fractionation in ALE ($69.07 \pm 8.95\%$) of AGS has contributed remarkably to the strong and elastic structure of AGS (Lin *et al.* 2010). Bacterial enzymes, as well as their genes and gene promoters, play important roles in alginate biosynthesis (Jain and Ohman 1998; Sautter *et al.* 2012). Interestingly, high osmolarity provided by NaCl (0.3 M) activates algC gene expression in *Pseudomonas*, which involves production of a key enzyme PMM that facilitates alginate biosynthesis (Zielinski *et al.* 1992). Thus, the presence of NaCl may also increase the number of alginate-like exopolysaccharides (ALE) in AGS through similar mechanisms. However, no relative studies have been conducted yet. Therefore, it is meaningful to examine whether the production of ALE in granules can be greatly accelerated while treating high salty wastewater. Accelerated ALE production will be greatly beneficial for reusing excess AGS as a potential biomaterial resource, as well as promoting the treatment of salty wastewater.

The influence of high salinity on AGS and its ALE formation was investigated in the present study. The main objectives were to evaluate the effect of high salinity on the characteristics of AGS, investigate the impact of high salinity on nutrients removal in AGS system, investigate the influence of high salinity on the amount and characteristics of ALE in AGS, and discuss the mechanism of salinity effect on ALE in AGS.

EXPERIMENTAL

Reactor Design and Operation

Three identical sequencing batch reactors (SBRs: R1, R2, and R3) with a working volume of 2 L were inoculated with 4.1 g/L of activated sludge taken from a local sewage treatment plant in Tianjin, China. The height and internal diameter of each reactor was 1 m and 0.06 m, respectively. The reactors were operated sequentially in a 4 h cycle at room temperature (25 ± 2 °C), with 2 min of influent filling, 30 min of non-aeration, 199 min of aeration, 4 min of settling, 2 min of decanting, and 3 min idling. Aeration was provided by an air pump (AL-60, Alita Industries, Inc., Baldwin Park, CA, USA) through air bubble diffusers at the bottom of each reactor with an air flow rate of 3.0 L/min, and the dissolved oxygen (DO) was maintained between 7 mg/L to 9 mg/L during aeration.

Synthetic Saline Sewage

The amount of biodegradable biomass in wastewater can be expressed as the chemical oxygen demand (COD). The synthetic wastewater used in this study was

composed of 600 mg COD/L (glucose and sodium acetate contributed to 50% of the total COD, respectively). The following chemicals were also used for the preparation of synthetic wastewater in this study (per L): 0.472 g $(\text{NH}_4)_2\text{SO}_4$, 0.030 g K_2HPO_4 , 0.023 g KH_2PO_4 , 0.300 g NaHCO_3 , 0.025 g $\text{MgSO}_4 \cdot 7\text{H}_2\text{O}$, 0.030 g CaCl_2 , and 0.020 g $\text{FeSO}_4 \cdot 7\text{H}_2\text{O}$. NaHCO_3 was added into the influent in order to maintain the influent pH at designated values (pH 7.5 to pH 8.0). Different amounts of salt (NaCl) were mixed with the synthetic wastewater to achieve final salinities of 0% (R1), 1% (R2), and 3% (R3) to the nearest percentage point, respectively.

Analytical Methods

The ammonia nitrogen ($\text{NH}_4\text{-N}$), nitrite nitrogen ($\text{NO}_2\text{-N}$), phosphorus ($\text{PO}_4\text{-P}$), mixed liquor (volatile) suspended solids (ML(V)SS), SVI, and COD were measured according to standard methods (APHA 2012). The pH was measured with a pH meter (HORIBA, Kyoto, Japan).

Extracellular polymeric substances (EPS) secreted by bacteria were calculated as the sum of proteins (PN) and polysaccharides (PS) in this study. The EPS was extracted from sludge by the formaldehyde and NaOH method (Adav and Lee 2011). The PN in the extracted EPS was determined using a quick Lowry method protein assay kit (LABAIDE, Shanghai, China), and the PS in the EPS was quantified by the anthrone-sulfuric acid method (DuBois *et al.* 1956).

The morphology characteristics and particle size of the seed sludge and granules in the reactor were observed using an optical microscope (SDPTOP, CX40, Ningbo Sunny Technology Co. Ltd, Yuyao, China) equipped with a digital camera (CANON, Tokyo, Japan). A scanning electron microscope (SEM, FEI-Quanta 200, Thermo Fisher Scientific, Waltham, MA, USA) was also used for the morphology observation. The strength of granules was estimated by using the increased turbidity in sludge sample supernatant after shaking at 2800 rpm on a vortex shaker (Kylin-Bell, Vortex-5, Haimen, China) for 2 min. The enzyme PMM1 and PMM2 of the granules was measured using ELISA kits (Chun Test Biological Technology, Shanghai, China) from the centrifugal supernatant after grinding the mixed granular sludge in a glass homogenizer. The Mg^{2+} in ALE was measured after sludge samples were extracted in Na_2CO_3 at 80 °C for 1 h. A 1 mL liquid sample was digested with 3 mL nitric acid (70%, Tianjin) at 100 °C for 1 h. The concentration was measured by inductively coupled plasma mass spectrometry (ICP-MS, ELAN DRC-e, Perkin Elmer, Waltham, MA, USA).

Alginate-like Exopolysaccharides (ALE) Extraction and Characterization

ALE extraction

Dried biomass (0.375 g) was homogenized for 3 min (FA25 High speed tissue homogenizer, Fluko, Shanghai, China) and extracted in 60 mL of 0.2 M Na_2CO_3 at 80 °C for 1 h. After centrifuging at $12850 \times g$ for 20 min, the pellet was discarded. The supernatant pH was adjusted to 2.2 by adding 1:4 HCl. The precipitate was collected by centrifugation ($12850 \times g$, 30 min), washed twice with deionized water, and dissolved in 0.1 M NaOH to obtain the ALE in sodium form (Lin *et al.* 2010; Felz *et al.* 2016). To accurately determine the amount of ALE, ALE liquid was measured by the carbazole method (Jain and Ohman 1998). Compared with the traditional gravimetric method, the carbazole method excludes impurities that affect the results. Briefly, 1 mL of the ALE sample was mixed with 5 mL of borate-sulfuric acid reagent (100 mM H_3BO_3 in concentrated H_2SO_4), and 0.15 mL of carbazole reagent (0.1% in ethanol) was added. The

mixture was heated at 100 °C for 15 min, and after cooling the absorbance at 530 nm was determined. The ALE concentrations were determined from a plot with sodium alginate (Meryer, Shanghai, China) as a standard.

The final ALE product was obtained by adding cold absolute ethanol to a final concentration of 80% (vol/vol) into the ALE in sodium form. The precipitate was collected by centrifugation (12850 g, 30 min), washed three times in absolute ethanol, and lyophilized.

Blocks fractionation

The ALE in sodium form (4.5 mL) was mixed with 0.5 mL of 4 M HCl and heated at 100 °C for 0.5 h. After cooling, the mixture was centrifuged (12850 × g, 30 min) and the supernatant solution was stored (MG blocks fraction). The insoluble material was dissolved in 0.1 M NaOH, the pH was decreased to 2.85 by the addition of 1.0 M HCl, and the soluble fraction was stored (MM blocks fraction). The insoluble fraction was dissolved by 0.1 M NaOH (GG blocks fraction). The ALE content of MG blocks, MM blocks, GG blocks fractions was determined by the carbazole method. The other blocks were determined by subtract the above blocks fractions from the total weight of the final ALE product.

Molecular weight (MW) distribution

The ALE samples were size-separated by ultrafiltration at 3, 50, and 100 kDa using Millipore membranes (Bedford, USA) in parallel mode. The collected solutions on each membrane were quantified by measuring the ALE content through carbazole method.

Gas Chromatography - Mass Spectrometry (GC-MS)

The ALE product was analyzed using a GC-MS system to detect the composition. Briefly, 10 mg final ALE product was added into 5 mL 1 M HCl /methanol, sealed, and heated at 85 °C for 24 h. After cooling, the mixture was neutralized with 100 mg Ag₂CO₃. The supernatant was collected by centrifugation (1000 × g, 3 min), the precipitate was washed twice, and all the supernatant combined and dried in a nitrogen atmosphere. Dried residue was trimethylsilylated by adding 2 mL of silylation reagent (pyridine/hexamethyldisilazane/chlorotrimethylsilane = 5:1:1) and fully mixed. The mixed sample was left to stand for 30 min and filtrated through a 0.22 μm membrane. The samples were analyzed with an Agilent 7890B GC/5977A MS device (Palo Alto, CA, USA). The GC separation was performed on a HP-5MS capillary column (30 m × 0.25 mm × 0.25 μm) (Agilent Technologies, Palo Alto, CA, USA). Split injection (10:1) was used at 280 °C with helium as a carrier gas at 1 mL/min, and the injection volume was 1 μL. The temperature program was as follows: 140 °C, hold for 2 min, increase at a rate of 8 °C/min to 250 °C, and then hold for 10 min. A solvent delay time of 3 min was performed before the ion source was turned on, and the mass spectra were acquired from 30 m/z to 550 m/z. The chromatographic peaks were identified using the NIST11 library (National Institute of Standards and Technology, Gaithersburg, MD, USA), and a match percentage was obtained by comparing the mass spectrum of a peak with that of a known compound from the library.

Microbial Community Analysis

The total DNA of granular sludge samples harvested on day 125 from R1, R2, and R3 were extracted by using a Mo-Bio Power Soil DNA Isolation Kit (MoBio Laboratories, Inc., Carlsbad, CA, USA) according to the manufacturer's protocol. After DNA extraction,

polymerase chain reaction (PCR) and high-throughput sequencing were performed by ALLWEGENE Inc. (Beijing, China).

To amplify the bacterial 16S rRNA gene, 338F (ACTCCTACGGGAGGCAGCA G) and 806R (GGACTACHVGGGTWTCTAAT) primers were used, targeting the V3-V4 region. Specific primers with barcodes and high-fidelity Fast Start Fastpfu DNA Polymerase (TransGen Biotech, Beijing, China) were used to conduct PCR. The PCR conditions were as follows: 95 °C for 5 min; 30 cycles consisting of 95 °C for 30 s; annealing at 56 °C for 30 s; elongation at 72 °C for 40 s; and a final extension step at 72 °C for 10 min. Samples were held at 4 °C afterwards.

After sequencing amplicons using a pair-end method by Illumina Mi Seq with a six-cycle index read, MOTHUR software based on MOTHUR SOP 454 pipelines (Schloss *et al.* 2011) was used for analyzing microbial biodiversity in the granules.

RESULTS AND DISCUSSION

Effect of Salinity on Characteristics of AGS

For the AGS system, the addition of salts can largely influence the morphological properties and physicochemical characteristics of granules. As shown in Table 1, there were differences in the granules in the three reactors with different concentrations of salts. Among these parameters, MLSS and SVI₃₀ were used to evaluate biomass growth and granular settling ability in the SBRs. After 130 days of operation, the MLSS in R2 and R3 were approximately 10.9 g/L and 13.4 g/L, which was much higher than that in R1 (6.6 g/L). In addition, granules in R2 and R3 had the lower SVI and larger wet sludge density (long term data of MLSS, MLVSS, and SVI are presented in Fig. S1). Thus, salinity greatly improved the total biomass content and settling ability, which could in turn promote nutrient removal and biomass separation.

Table 1. Physical Characteristics of Granules in the Reactors on Day 130

Parameters	R1	R2	R3
MLSS (g/L)	6.6	10.9	13.4
MLVSS (g/L)	6.0	9.6	11.8
SVI ₃₀ (mL/g)	54.2	32.9	12.0
mean diameter (mm)	1.5	1.8	0.8
wet sludge density (g/mL)	1.03	1.04	1.07
turbidity increase (FAU/g VSS)	44.6	10.9	28.2

The particle size of the granules was also investigated (Table 1). The average diameter of granules in R2 was about 1.8 mm after 130 days of cultivation, which was larger than that of granules in R1 (1.5 mm) and R3 (0.8 mm). Also the particle sizes of larger areas around 1-2 mm, 2-3mm, and >3 mm in R2 were all observed to have the largest percentages (Fig. S2). The granule size influences the nutrient removal process. Larger granules in R2 had enriched stratified structure, which was in favor of nutrient removal, but small granules in R3 had insufficient stratified structure, which may lead to unsatisfactory nutrient removal (Corsino *et al.* 2017). On day 130 (Fig. 1, Fig. S2a-c), the particle surface of granules in R2 was smoother than in R1 and R3, and the granules in R2 had more regular shapes of sphericity. By contrast, granules in R3 had rugged surfaces, and surface of the granules in R1 was incompact and loose with irregular sphere shape.

SEM observations also showed that the granules had a more compact and denser structures in R2 and R3 than R1 (Fig. S3). This might be related to the enlarged sludge density in the presence of salinity.

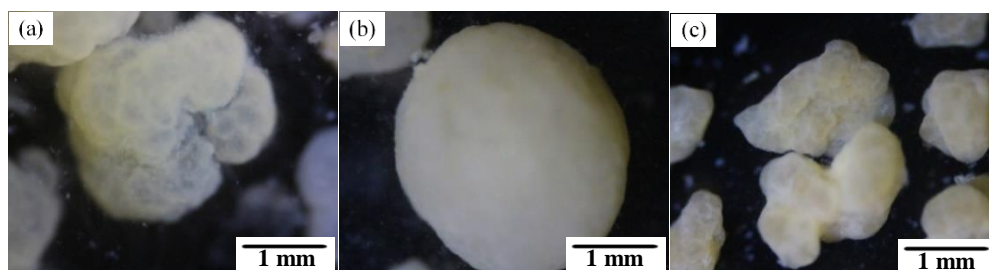


Fig. 1. Digital images of granules in R1 (a), R2 (b), and R3 (c) on day 130: R1, the reactor fed with normal wastewater; R2, the reactor fed with 1% salinity wastewater; R3, the reactor fed with 3% salinity wastewater

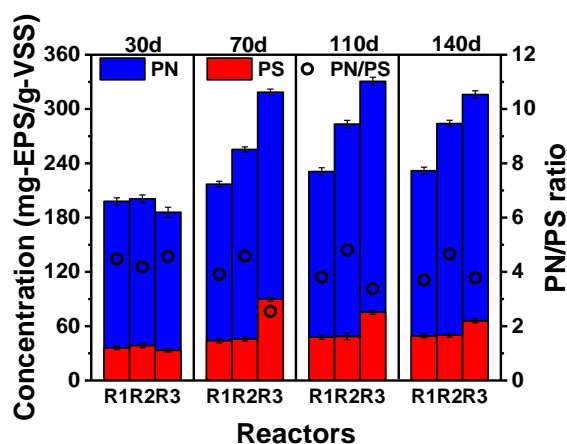


Fig. 2. Variation of EPS during the cultivation

Extracellular polymeric substances (EPS) are secreted by bacteria and contribute to the granular structure and granulation process in AGS. In addition, EPS are known to contribute to sludge flocculation, settling, dewatering, metal binding and removal of toxic organic compounds (Nouha *et al.* 2017). Essential constituents of EPS are PN and PS, and a higher ratio of PN/PS enhances the granular stability (Ahmad *et al.* 2017). Figure 2 shows the production and composition of EPS in granules after 30, 70, 110, and 140 days in all SBARs. Total EPS and PN production increased with increased salinity. This might have been due to a large quantity of exoenzymes produced in the presence of salinity (Wang *et al.* 2015). The increased EPS at high salinities might have resulted in the enhanced settling ability of AGS; thus the AGS in R2 and R3 had lower SVI and larger wet sludge density (Table 1). The PS content in R1 and R2 stayed relatively stable at different times. In R3, PS content increased greatly after the addition of 3% salinity, which might have been because PS in the EPS could help granules survive under sodium toxicity (Wan *et al.* 2014). The PS decreased with time in R3 because of the granules' adaption to the salinity. Moreover, the PN/PS ratio was highest in R2, which could enhance granular strength in R2. As shown in Table 1, granular sludge in R2 had the highest granular strength (lowest supernatant turbidity change of 10.9 FAU/g VSS after shaking; R1: 44.6 FAU/g VSS; R3: 28.2 FAU/g VSS).

Therefore, a salinity of 1% greatly improved the characteristics of granular sludge in R2. Larger particle size, smooth spheroidicity shape, and enhanced granular strength were obtained in R2. Granules in R2 also had higher PN/PS ratios of EPS, which could improve the granule stability (Ahmad *et al.* 2017).

Effect of Salinity on Nutrients Removal of AGS System

As shown in Fig. S4a, at high salinities of 1% and 3%, the effluent TOC in R2 and R3 had stable concentrations of about 5 mg/L to 10 mg/L, with no obvious deterioration of the substrate. In addition, ammonia oxidizing efficiency showed no remarkable difference at high salinity, except in the R3 reactor, where there was suppression at the initial stage because of the high salinity. The effluent $\text{NH}_4\text{-N}$ in the R3 reactor had a sudden increase from 40 days to 70 days (Fig. S4b), but it decreased to almost zero afterwards. However, the $\text{NO}_2\text{-N}$ concentration in R3 began to accumulate with the salt addition and reached about 14 mg/L after 70 days (Fig 3a). There was no obvious accumulation in R1 and R2, with only small fluctuations; the value became nearly zero after 80 days. The accumulation of $\text{NO}_2\text{-N}$ concentration in R3 might have been because nitrite oxidizing bacteria (NOB) were inhibited at the high salinity of 3% (Wan *et al.* 2014).

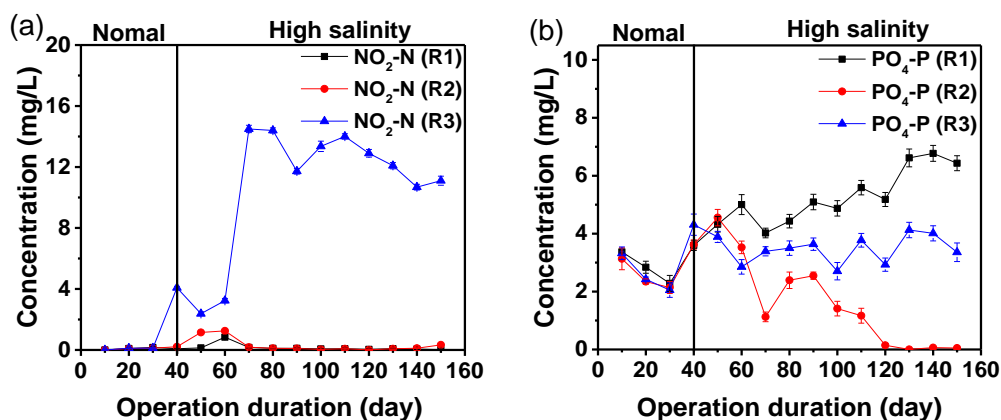


Fig. 3. Variation of $\text{NO}_2\text{-N}$ (a) and $\text{PO}_4\text{-P}$ (b) in the effluent during the cultivation

The P removal efficiency was greatly improved in the presence of salinity (Fig. 3b). The largest P removal was observed in R2, and the effluent $\text{PO}_4\text{-P}$ concentration in R2 declined to 0.1 mg/L on day 150. It remained at 6.4 mg/L in R1 and 3.4 mg/L in R3. The presence of moderate NaCl (1%) induced the improvement of P removal, and the excessive NaCl induced the drop of the P removal (3%). AGS is known to have three layers (aerobic, anoxic, anaerobic), among which the inner part of anaerobic layer is more fit for the living of polyphosphate accumulating organisms (PAOs), which are profitable for P removal (Corsino *et al.* 2015). A moderate salinity of 1% could enhance the anaerobic metabolism for maintenance energy production in PAOs, while in the higher range of salinity over 2% the metabolism rate decreased (Welles *et al.* 2014). Thus the AGS in R2 had higher P removal efficiency than R1 and R3.

Therefore, the substrate degradation and ammonia oxidizing did not decrease in the presence of salinity, except for $\text{NO}_2\text{-N}$ accumulation which happened in 3% salinity. In contrast, P removal efficiency was largely enhanced in the presence of salinity, especially in 1% salinity. Salinity of 3% (R3) had less improvement for P removal than 1% salinity (R2), but still largely enhanced compared to no salt condition (R1).

Effects of Salinity on Alginate-Like Exopolysaccharides

Alginate-like exopolysaccharides amount

The ALE concentration extracted from granules of the three SBRs was detected during the experiment. Figure 4 shows that the amount of ALE increased with the cultivation time in all reactors. The original sludge had roughly 13 mg ALE/g VSS, and cultivation increased the amount of ALE in all three reactors. After the addition of different concentrations of salts, the increase in the amount of ALE in R1 (0% salinity) and R3 (3% salinity) stopped at about 60 days, while the ALE amount in R2 (1% salinity) continued increasing until about 110 days. Finally, the amount of ALE in R2 reached 49.8 mg/g VSS at 140 days, which was much higher than in R1 (26.8 mg/g VSS) and R3 (28.9 mg/g VSS). The results showed that the salinity of 1% in the synthetic saline sewage could greatly accelerate the ALE formation in granular sludge. This might have been because moderate salinity could motivate the expression of gene *algC*, which involves ALE production, but excessive salinity might not motivate it or even could inhibit it (Zielinski *et al.* 1992).

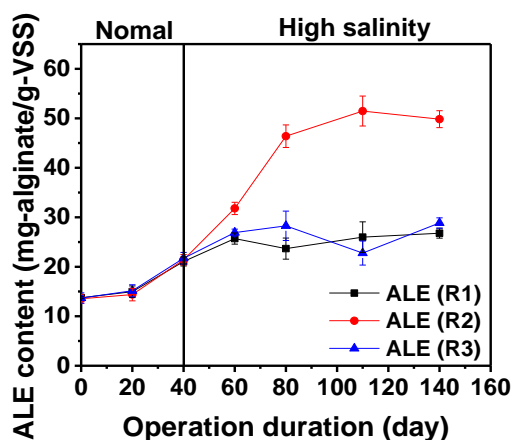


Fig. 4. Variation amount of ALE during the cultivation

Osmotic stress is an important environmental factor that influences the alginate production in the bacteria *Pseudomonas aeruginosa*, because the level of the *algC* gene expression can improve while the medium osmolarity (*i.e.*, the NaCl or sucrose concentration) increases (May *et al.* 1991; Zielinski *et al.* 1992). Phosphomannomutase (PMM) is the product of the *algC*, which can play an important role in the alginate synthesizing process (Jain and Ohman 1998). The role of PMM is to catalyze the interconversion between mannose-6-phosphate (M6P) and mannose-1-phosphate (M1P), which are both key precursors of alginate synthesizing (Fig. 5) (May *et al.* 1991; Yu *et al.* 2015). Zielinski *et al.* (1992) has reported that the maximum activation to *algC* expression was achieved at 0.3 M NaCl, and a higher concentration of NaCl would result in decreased activation. Thus, it could be assumed that *algC* could also play an important role on enhancing the production of alginate-like exopolysaccharides (ALE) through synthesizing more PMM, especially while osmotic pressure increased. PMM1 and PMM2 are two isoforms of PMM, which have similar sequence and gene structure, and may have the same origin before mammalian radiation (Schollen *et al.* 1998; Heykants *et al.* 2001). As shown in Table 2, both PMM1 and PMM2 of the granule interstitial fluid in R2 were much higher than in R1 and R3. PMM1 and PMM2 improved in 1% salinity, but did not show any increase in 3% salinity. It was found that osmolarity in R2 provided by 1% NaCl favored

the gene *algC* expression in the granules, and thus the enzyme product PMM increased as well as the final product ALE in the synthesizing process (Fig. 5). However, activation of gene *algC* disappeared when salinity increased to 3%, so ALE in 3% salinity granule did not show any increase.

Table 2. Amount of Phosphomannomutase in Granules on Day 50

Phosphomannomutase	R1	R2	R3
PMM1 (U/g VSS)	1.9 ± 0.1	3.3 ± 0.2	1.8 ± 0.2
PMM2 (ng/g VSS)	4.1 ± 0.1	5.4 ± 0.3	3.3 ± 0.2

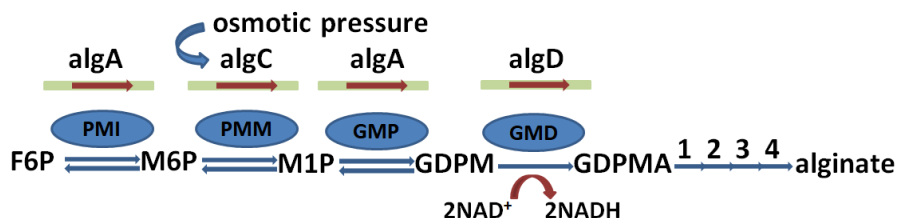


Fig. 5. Mechanism for ALE activation by osmolarity in alginic acid biosynthetic pathway of bacteria. Arrows 1, 2, 3, and 4 indicate the undefined steps of polymerization, acetylation, export, and epimerization. The gene encoding each enzyme is indicated above the enzyme name. PMI, phosphomannose isomerase; PMM, Phosphomannomutase; GMP, GDP-mannose pyrophosphorylase; GMD, GDP-mannose-dehydrogenase; F6P, Fructose 6-phosphate; M6P, mannose 6-phosphate; M1P, mannose 1-phosphate; GDPM, GDP-mannose; GDPMA, GDP-mannuronic acid (May et al. 1991; Jain and Ohman 1998)

Alginate-like exopolysaccharides fractionation

Alginate is an important hydrogel material, and its mechanical properties (gel-forming capacity and viscoelasticity) are very important for its application in different fields (Lin *et al.* 2013). The mechanical properties of alginate gels are typically enhanced by increasing the length of G-block and the molecular weight (Lee and Mooney 2012). Therefore, blocks fractionation and molecular weight (MW) distribution were performed to characterize the mechanical properties of ALE. Figure 6a shows that the proportion of GG blocks in ALE was largely increased from 2.2 mg/g-VSS in R1 to 22.8 mg/g-VSS in R2 while it decreased to 1.6 mg/g-VSS in R3, which showed a larger gel-forming capacity in R2 with 1% salinity (Lin *et al.* 2013). This might be because the presence of NaCl could result in the loss of Mg^{2+} in granules (Wan *et al.* 2014) and thus the increase of GG blocks of ALE could help to bind more Mg^{2+} to ease their deficiency and maintain their growth need. As it is known, the guluronic acid (G-block) content of alginate has an affinity for divalent cations (Davis *et al.* 2003). While in the presence of an excessive concentration of NaCl (3%), overproduction of GG-block might be inhibited due to the toxicity of sodium ions to alginate relative genes or enzymes. The Mg^{2+} present in the ALE was 1.4 mg/g VSS, 1.5 mg/g VSS, and 1.0 mg/g VSS in R1, R2, and R3, respectively. The ALE in R2 had the highest Mg^{2+} due to the enlarged GG block fractionation.

As shown in Fig. 6b, ALE had a broad spectrum of MW in all reactors, while ALE in R2 had the largest part of high MW molecules (MW > 100 kDa). The percentages of ALE with MW < 3 kDa, 3 kDa to 50 kDa, and 50 kDa to 100 kDa, were only 0%, 1.1%, and 1.4%, in R2, respectively, which were much lower than those in R1 (3.3%, 4.6%, 13.9%) and R3 (0%, 8.0%, 5.9%). However, the percentage of ALE part with MW > 100 kDa was 97.5% in R2, which was much higher than in R1 (78.3%) and R3 (86.1%). Thus,

the ALE in R2 had larger MW than in either R1 or R3. The larger MW might have resulted from the increasing of G-blocks, as a high concentration of polyguluronic acid residues had specificity for divalent cations due to its “egg-box” structure. This structure also involved many single guluronic acid chains combined together to form a larger molecule network (Davis *et al.* 2003). Therefore, ALE in R2 (1% salinity) showed the largest GG block fractionation and MW, which showed that it possessed the most enhanced mechanical properties. Furthermore, these enhanced properties might contribute to the strong performance of the AGS granules in wastewater treatment, including its stability and nutrients removal efficiency.

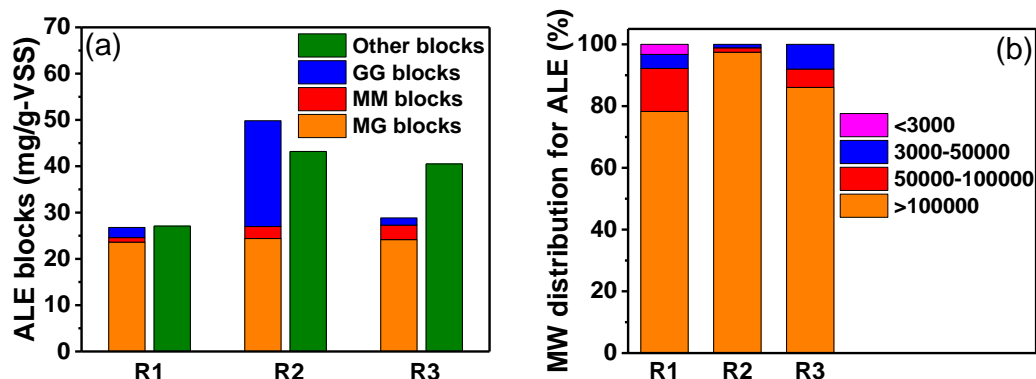


Fig. 6. Blocks fractionation (a) and MW distributions (b) of ALE in granules of R1, R2, and R3

Alginate-like exopolysaccharides composition analysis

For the obtained ALE, varieties of compounds might be present inside, and different compositions could lead to different properties in the ALE product. Compositions were detected through gas chromatography mass spectrometry (GC-MS). Figure S5 shows the compounds identified in the standard alginate (extracted from brown algae), and very few mannuronic acid (M) and guluronic acid (G) monomers could be detected, as this detecting method of GC-MS might mainly focus on the other compounds in the ALE besides the pure alginate. Figure 7 shows the compounds identified by GC-MS in the ALE. Approximately 36, 38, and 32 methyl and silane derivatives were identified in R1, R2, and R3, respectively (Table S1, S2, S3). The solid ALE extracted from the granules was composed of various compounds with a complex polymer combination besides the pure alginate.

Galactoside was the largest portion in all reactors, and the portion of Galactoside in R3 (47.3%) was much higher than R1 (26.2%) and R2 (26.0%). However, D-(+)-Glucosamine accounted for 17.1% in R2, which was much higher than in R1 (10.9%) and R3 (7.5%). Glucosamine is widely used as a dietary supplement by patients who suffer from osteoarthritis, and it is expected to have an important role in cancer treatment (Zahedipour *et al.* 2017). Thus, enrichment in the ALE of R2 granules may contribute to the use of ALE as a potential source for medicine.

Lipid content, including esters (L-alaninate, Phosphoric acid propyl ester) and fatty acids (Palmitic Acid, Hexadecanoate), accounted for 6.3% in ALE of R2, which was much higher than in R1 (0.9%) and R3 (1.0%). The larger content of lipids in the ALE of R2 could induce a stronger water-barrier property. Moreover, larger enrichment of an octadecanamide derivative (Octadecanamide, N-nitroso-), was observed in the ALE of R2 (4.2%), while this content was only 0% and 0.6% in R1 and R3, respectively.

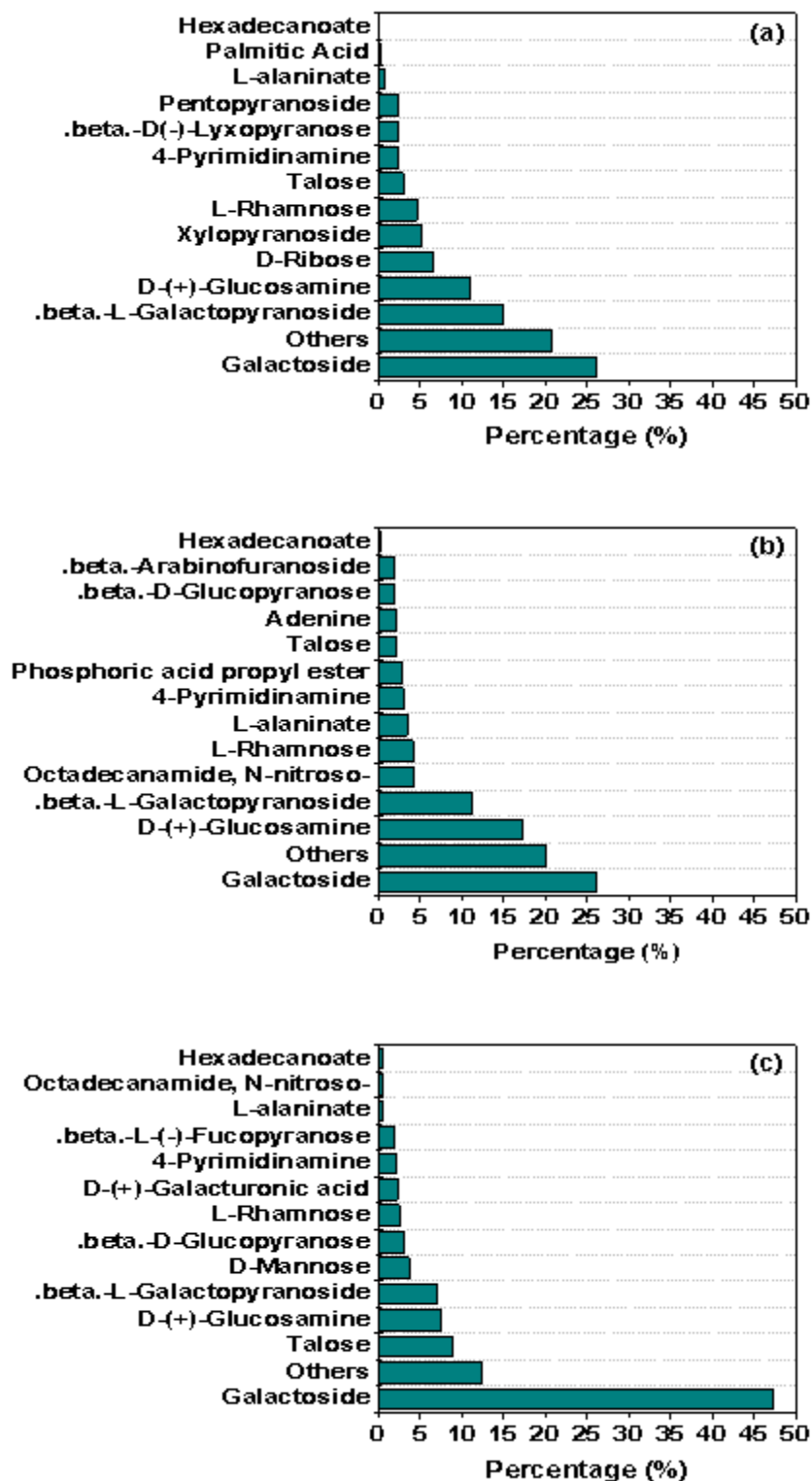


Fig. 7. GC-MS analysis for the solid ALE compositions in the AGS of (a) R1; (b) R2; and (c) R3

Octadecanamide can reduce the friction coefficients of products, which is beneficial for extrusion, injection molding, and compression molding of related products (Lv *et al.* 2009). Therefore, the enrichment of glucosamine, lipid content, and octadecanamide derivative in ALE of R2 gave it potential use in medicine, stronger water-barrier property, and a reduction of the friction coefficients of products.

Microbial Community Analysis

EPS and ALE are both the products of microbial metabolism and decay. Therefore, the noticeable differences in the accumulation, characteristics, and composition of ALE among R1, R2, and R3 reactors might exist because of the different microbial communities in the three reactors. As shown in Fig. 8a, the predominant bacteria covered Chlorobi, Bacteroidetes (Cytophagia, Flavobacteria, and Sphingobacteria), Nitrospirae, and Proteobacteria (Alphaproteobacteria, Betaproteobacteria, Gammaproteobacteria, and Deltaproteobacteria), which accounted for 89.5%, 94.3%, and 89.7% in the granules of R1, R2, and R3 reactors, respectively.

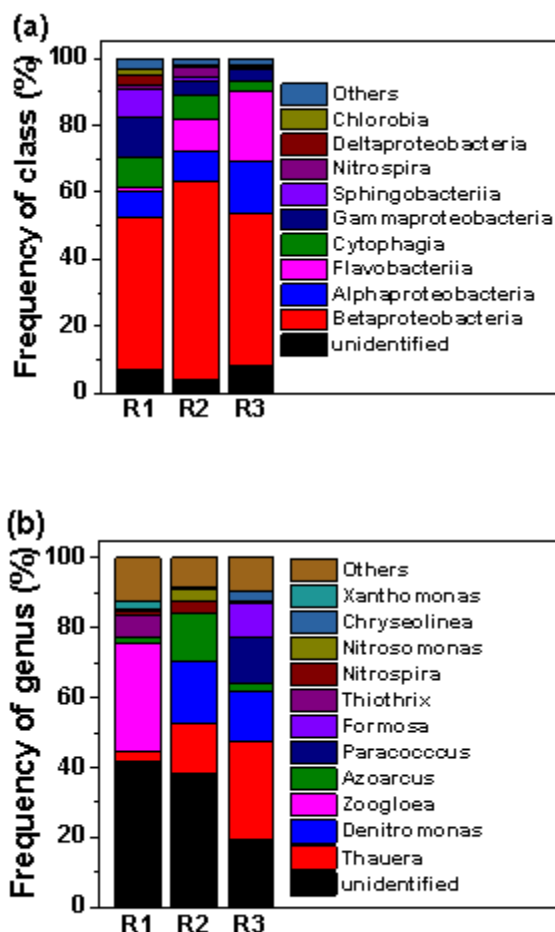


Fig. 8. Abundance of main classes (a) and genera (b) in the granules from R1, R2, and R3 on day 125

The amount of ALE in AGS is likely related to some specific bacteria, which possibly belong to the phylum Proteobacteria. The phylum Proteobacteria has the largest phylogenetic composition, containing 116 validated bacterial families (Shin *et al.* 2015)

and some alginate-producing bacteria. Only the *Pseudomonas* and *Azotobacter* have been discovered to produce alginate (Flores *et al.* 2013; Yang *et al.* 2014), which belong to phylum Proteobacteria. Granules enriched with Proteobacteria can also produce ALE (Pronk *et al.* 2015). Therefore, the portion of Proteobacteria was important in these three reactors. Proteobacteria occupied the largest portion of the bacteria in the three reactors, which was about 68.1%, 73.1%, and 65.6% in R1, R2, and R3, respectively. The percentage of proteobacteria was largest in R2, but lowest in R3. The results indicated that salinity of 1% in R2 enriched these bacteria, while higher salinity of 3% in R3 showed the inhibition. This might also be a reason for improvement of ALE in R2 compared with R1 and R3.

Besides the ALE production, the performance of AGS system and EPS content might also relate to some certain bacteria. Among the Proteobacteria, Betaproteobacteria in R2 accounted for 59.2%, which was also much higher than in R1 (45.6%) and R3 (45.5%). However, the Alphaproteobacteria quantity in R3 accounted for 15.7%, which was higher than that in R1 (7.8%) and R2 (9.3%). This may be because Alphaproteobacteria has a diverse range of metabolic capacities, so it became abundant at high salinity while Betaproteobacteria disappeared in contrast (Ramos *et al.* 2015). Many bacteria belonging to Betaproteobacteria could enhance the performance of the AGS system. *Azoarcus*, *Denitromonas*, and *Nitrosomonas* are regarded to be closely correlated with strong biodegradation and nitrogen removal (Hurek and Reinhold-Hurek 2003; Lew *et al.* 2012; Huang *et al.* 2014). Therefore, the enriched bacteria in R2 (Fig. 8b) could enhance the nutrition (COD and N) removal. Also, *Rhodocyclus*-related bacteria are regarded as important to P removal in activated sludge (Zengin *et al.* 2011). As shown in Fig. S6, bacteria belonging to family Rhodocyclaceae had higher content in R2 (55.9%) and R3 (44.7%) than in R1 (36.1%), which was in agreement with the enhancement of P removal in R2 and R3. Genus *Thauera* has been regarded to be closely related with EPS (Huang *et al.* 2014). *Thauera* content increased with increases of concentration of salinity, and was 3.0%, 14.3%, and 28.6% in R1, R2, and R3, respectively (Fig. 8b). Therefore, EPS also increased with the salinity due to the increased population of *Thauera* as one of the explanations (Fig. 2).

Additionally, *Nitrospira*, which belonged to Nitrospirae, was 1.2%, 3.4%, and 0.04% in R1, R2, and R3, respectively (Fig. 8b). The lack of *Nitrospira* in R3 could result in the NO₂-N accumulating because it was related to the nitrite oxidizing to nitrate (Daims and Wagner 2018). Moreover, Flavobacteria accounted for 20.7% in R3 (Fig. 8a), which was much higher than in R1 (0.7%) and R2 (9.4%) because Flavobacteria were common in high salinity areas, such as oceans and coastal waters (Hahnke and Harder 2013).

Therefore, the microbial community was affected by different concentrations of salt. Proteobacteria was enriched by 1% salinity in R2, which was beneficial for ALE enrichment. Moreover, many enriched Betaproteobacteria at high salinity could play important roles in AGS. *Azoarcus*, *Denitromonas*, and *Nitrosomonas* were beneficial for improving nutrient and nitrogen removal in R2, Rhodocyclaceae was useful for enhancing P removal in R2 and R3, and *Thauera* was good for useful EPS in R2 and R3.

Mechanism

The salt activation mechanism of ALE produced in 1% salinity was proposed as follows. First, moderate osmotic pressure could largely accelerate the gene *algC* expression, the product of which was PMM, a key enzyme in the ALE synthesizing process. The PMM content in AGS of R2 increased, which induced the increasing amount of ALE. While at excessive osmotic pressure provided by 3% salinity, the activation to

algC expression decreased, so the amount of ALE showed a large drop in R3. Second, 1% salinity could enrich Proteobacteria in R2, which was good for ALE enrichment.

As a hydrogel material in AGS, ALE might play an important role in enhancing the performance of AGS systems. ALE can help maintain the granule stability, and also increase the settling ability of AGS *via* entrapping more protein in EPS (Lin *et al.* 2010; Datta *et al.* 2013).

CONCLUSIONS

1. Larger particle size, smooth spheroidicity shape, and enhanced granular strength in R2 was induced by 1% salinity.
2. Salinities of 1% and 3% in R2 and R3 did not affect the removal of TOC and ammonia, and largely enhanced the P removal.
3. The ALE were largely enriched in the moderate concentration of 1% salinity, and the amount of ALE in R2 reached 49.8 mg/g VSS at 140 days, which was much higher than in R1 (26.8 mg/g VSS) and R3 (28.9 mg/g VSS). The largest GG block fractionation and MW of ALE was shown in R2, which indicated that it possessed the most enhanced mechanical properties. A 1% salinity enriched the glucosamine, lipid content, and octadecanamide derivative in ALE of R2, which involved medicinal potential, stronger water-barrier property, and reduction of the products' friction coefficients.
4. Proteobacteria was enriched in 1% salinity, which was good for ALE enrichment in R2. Moreover, *Azoarcus*, *Denitromonas*, and *Nitrosomonas* were good for improving nutrient and nitrogen removal in R2. Rhodocyclaceae was effective for enhancing P removal in R2 and R3, and *Thauera* was effective in enlarging EPS in R2 and R3.

ACKNOWLEDGMENTS

The authors would like to thank the financial support from the National Natural Science Foundation of China (No. 51608279) and the Tianjin Municipal Science and Technology Project (No. 17ZXSTSF00100).

REFERENCES CITED

- Adav, S. S., and Lee, D.-J. (2011). "Characterization of extracellular polymeric substances (EPS) from phenol degrading aerobic granules," *J. Taiwan Inst. Chem. Eng.* 42(4), 645-651. DOI: 10.1016/j.jtice.2010.11.012
- Ahmad, J. S. M., Cai, W., Zhao, Z., Zhang, Z., Shimizu, K., Lei, Z., and Lee, D.-J. (2017). "Stability of algal-bacterial granules in continuous-flow reactors to treat varying strength domestic wastewater," *Bioresour. Technol.* 244(1), 225-233. DOI: 10.1016/j.biortech.2017.07.134
- American Public Health Association (APHA) (2012). *Standard Methods for the Examination of Water and Wastewater*, 20th Ed., Washington, D.C.
- Borazjani, N. J., Tabarsa, M., You, S., and Rezaei, M. (2017). "Effects of extraction methods on molecular characteristics, antioxidant properties and immunomodulation

- of alginates from *Sargassum angustifolium*,” *Int. J. Biol. Macromol.* 101, 703-711. DOI: 10.1016/j.ijbiomac.2017.03.128
- Corsino, S. F., Campo, R., Bella, G. D., Torregrossa, M., and Viviani, G. (2015). “Cultivation of granular sludge with hypersaline oily wastewater,” *Int. Biodeterior. Biodegrad.* 105, 192-202. DOI: 10.1016/j.ibiod.2015.09.009
- Corsino, S. F., Capodici, M., Torregrossa, M., and Viviani, G. (2017). “Physical properties and extracellular polymeric substances pattern of aerobic granular sludge treating hypersaline wastewater,” *Bioresour. Technol.* 229, 152-159. DOI: 10.1016/j.biortech.2017.01.024
- Daims, H., and Wagner, M. (2018). “Nitrospira,” *Trends Microbiol.* 26(5), 462-463. DOI: 10.1016/j.tim.2018.02.001
- Datta, S., Christena, L. R., and Rajaram, Y. R. (2013). “Enzyme immobilization: An overview on techniques and support materials,” *3 Biotech* 3(1), 1-9. DOI: 10.1007/s13205-012-0071-7
- Davis, T. A., Volesky, B., and Mucci, A. (2003). “A review of the biochemistry of heavy metal biosorption by brown algae,” *Water Res.* 37(18), 4311-4330. DOI: 10.1016/S0043-1354(03)00293-8
- Díaz-Barrera, A., Aguirre, A., Berrios, J., and Acevedo, F. (2011). “Continuous cultures for alginate production by *Azotobacter vinelandii* growing at different oxygen uptake rates,” *Process Biochem.* 46(9), 1879-1883. DOI: 10.1016/j.procbio.2011.06.022
- DuBois, M., Gilles, K. A., Hamilton, J. K., Rebers, P. A., and Smith, F. (1956). “Colorimetric method for determination of sugars and related substances,” *Anal. Chem.* 28(3), 350-356. DOI: 10.1021/ac60111a017
- Felz, S., Al-Zuhairy, S., Aarstad, O. A., van Loosdrecht, M. C. M., and Lin, Y. M. (2016). “Extraction of structural extracellular polymeric substances from aerobic granular sludge,” *J. Vis. Exp.* 115. DOI: 10.3791/54534
- Flores, C., Moreno, S., Espín, G., Peña, C., and Galindo, E. (2013). “Expression of alginases and alginate polymerase genes in response to oxygen, and their relationship with the alginate molecular weight in *Azotobacter vinelandii*,” *Enzyme Microb. Tech.* 53(2), 85-91. DOI: 10.1016/j.enzmictec.2013.04.010
- Hahnke, R. L., and Harder, J. (2013). “Phylogenetic diversity of *Flavobacteria* isolated from the North Sea on solid media,” *Syst. Appl. Microbiol.* 36(7), 497-504. DOI: 10.1016/j.syapm.2013.06.006
- He, Q., Zhang, W., Zhang, S., Zou, Z., and Wang, H. (2017). “Performance and microbial population dynamics during stable operation and reactivation after extended idle conditions in an aerobic granular sequencing batch reactor,” *Bioresour. Technol.* 238, 116-121. DOI: 10.1016/j.biortech.2017.03.181
- Heykants, L., Schollen, E., Grünewald, S., and Matthijs, G. (2001). “Identification and localization of two mouse phosphomannomutase genes, Pmm1 and Pmm2,” *Gene* 270(1-2), 53-59. DOI: 10.1016/S0378-1119(01)00481-4
- Huang, W., Wang, W., Shi, W., Lei, Z., Zhang, Z., Chen, R., and Zhou, B. (2014). “Use low direct current electric field to augment nitrification and structural stability of aerobic granular sludge when treating low COD/NH₄-N wastewater,” *Bioresour. Technol.* 171, 139-144. DOI: 10.1016/j.biortech.2014.08.043
- Hurek, T., and Reinhold-Hurek, B. (2003). “*Azoarcus* sp. strain BH72 as a model for nitrogen-fixing grass endophytes,” *J. Biotechnol.* 106, 169-178. DOI: 10.1016/j.jbiotec.2003.07.010
- Jain, S., and Ohman, D. E. (1998). “Deletion of algK in mucoid *Pseudomonas*

- aeruginosa* blocks alginate polymer formation and results in uronic acid secretion,” *J. Bacteriol.* 180(3), 634-641.
- Jorfi, S., Pourfadakari, S., and Ahmadi, M. (2017). “Electrokinetic treatment of high saline petrochemical wastewater: Evaluation and scale-up,” *J. Environ. Manage.* 204(1), 221-229. DOI: 10.1016/j.jenvman.2017.08.058
- Lee, K. Y., and Mooney, D. J. (2012). “Alginate: Properties and biomedical applications,” *Prog. Polym. Sci.* 37(1), 106-126. DOI: 10.1016/j.progpolymsci.2011.06.003
- Lew, B., Stief, P., Beliavski, M., Ashkenazi, A., Svitlica, O., Khan, A., Tarre, S., de Beer, D., and Green, M. (2012). “Characterization of denitrifying granular sludge with and without the addition of external carbon source,” *Bioresource Technol.* 124, 413-420. DOI: 10.1016/j.biortech.2012.08.049
- Liang, Y., Zhu, H., Bañuelos, G., Yan, B., Shutes, B., Cheng, X., and Chen, X. (2017). “Removal of nutrients in saline wastewater using constructed wetlands: Plant species, influent loads and salinity levels as influencing factors,” *Chemosphere* 187, 52-61. DOI: 10.1016/j.chemosphere.2017.08.087
- Lin, Y. M., de Kreuk, M., van Loosdrecht M. C. M., and Adin, A. (2010). “Characterization of alginate-like exopolysaccharides isolated from aerobic granular sludge in pilot-plant,” *Water Res.* 44(11), 3355-3364. DOI: 10.1016/j.watres.2010.03.019
- Lin, Y. M., Nierop, K. G. J., Girbal-Neuhauser, E., Adriaanse, M., and van Loosdrecht, M. C. M. (2015). “Sustainable polysaccharide-based biomaterial recovered from waste aerobic granular sludge as a surface coating material,” *Sustainable Mater. Technol.* 4, 24-29. DOI: 10.1016/j.susmat.2015.06.002
- Lin, Y. M., Sharma, P. K., and van Loosdrecht, M. C. M. (2013). “The chemical and mechanical differences between alginate-like exopolysaccharides isolated from aerobic flocculent sludge and aerobic granular sludge,” *Water Res.* 47(1), 57-65. DOI: 10.1016/j.watres.2012.09.017
- Lv, G., Wang, L., Liu, J., and Li, S. (2009). “Method for determination of fatty acid amides in polyethylene packaging materials—Gas chromatography/mass spectrometry,” *J. Chromatogr. A* 1216(48), 8545-8548. DOI: 10.1016/j.chroma.2009.10.008
- May, T. B., Shinabarger, D., Maharaj, R., Kato, J., Chu, L., Devault, J. D., Roychoudhury, S., Zielinski, N. A., Berry, A., and Rothmel, R. K. (1991). “Alginate synthesis by *Pseudomonas aeruginosa*: A key pathogenic factor in chronic pulmonary infections of cystic fibrosis patients,” *Clin. Microbiol. Rev.* 4(2), 191-206.
- Morais, I. L. H., Silva, C. M., Zanuncio, J. C., and Zanuncio, A. J. V. (2018). “Structural stabilization of granular sludge by addition of calcium ions into aerobic bioreactors,” *BioResources* 13(1), 176-191. DOI: 10.15376/biores.13.1.176-191
- Nouha, K., Kumar, R. S., Balasubramanian, S., and Tyagi, R. D. (2017). “Critical review of EPS production, synthesis and composition for sludge flocculation,” *J. Environ. Sci.* 66, 225-245. DOI: 10.1016/j.jes.2017.05.020
- Pan, Y., Zhou, M., Cai, J., Li, X., Wang, W., Li, B., Sheng, X., and Tang, Z. (2018). “Significant enhancement in treatment of salty wastewater by premagnetization Fe⁰/H₂O₂ process,” *Chem. Eng. J.* 339, 411-423. DOI: 10.1016/j.cej.2018.01.017
- Peña, C., Millán, M., and Galindo, E. (2008). “Production of alginate by *Azotobacter vinelandii* in a stirred fermentor simulating the evolution of power input observed in shake flasks,” *Process Biochem.* 43(7), 775-778. DOI: 10.1016/j.procbio.2008.02.013
- Pronk, M., Abbas, B., Kleerebezem, R., and van Loosdrecht, M. C. M. (2015). “Effect of

- sludge age on methanogenic and glycogen accumulating organisms in an aerobic granular sludge process fed with methanol and acetate,” *Microb. Biotechnol.* 8(5), 853-864. DOI: 10.1111/1751-7915.12292
- Ramos, C., Suárez-Ojeda, M. E., and Carrera, J. (2015). “Long-term impact of salinity on the performance and microbial population of an aerobic granular reactor treating a high-strength aromatic wastewater,” *Bioresource Technol.* 198, 844-851. DOI: 10.1016/j.biortech.2015.09.084
- Saude, N., Chèze-Lange, H., Beunard, D., Dhulster, P., Guillochon, D., Cazé, A.-M., Morcellet, M., and Junter, G.-A. (2002). “Alginate production by *Azotobacter vinelandii* in a membrane bioreactor,” *Process Biochem.* 38(2), 273-278. DOI: 10.1016/S0032-9592(02)00090-0
- Sautter, R., Ramos, D., Schneper, L., Ciofu, O., Wassermann, T., Koh, C.-L., Heydorn, A., Hentzer, M., Høiby, N., Kharazmi, A., Molin, S., DeVries, C. A., Ohman, D. E., and Mathee, K. (2012). “A complex multilevel attack on *Pseudomonas aeruginosa* algT/U expression and AlgT/U activity results in the loss of alginate production,” *Gene* 498(2), 242-253. DOI: 10.1016/j.gene.2011.11.005
- Schloss, P. D., Gevers, D., and Westcott, S. L. (2011). “Reducing the effects of PCR amplification and sequencing artifacts on 16S rRNA-based studies,” *PLoS One* 6(12). DOI: 10.1371/journal.pone.0027310
- Schollen, E., Pardon, E., Heykants, L., Renard, J., Doggett, N. A., Callen, D. F., Cassiman, J.-J., and Matthijs, G. (1998). “Comparative analysis of the phosphomannomutase genes PMM1, PMM2 and PMM2Ψ: The sequence variation in the processed pseudogene is a reflection of the mutations found in the functional gene,” *Hum. Mol. Genet.* 7(2), 157-164. DOI: 10.1093/hmg/7.2.157
- Shin, N.-R., Whon, T. W., and Bae, J.-W. (2015). “Proteobacteria: Microbial signature of dysbiosis in gut microbiota,” *Trends Biotechnol.* 33(9), 496-503. DOI: 10.1016/j.tibtech.2015.06.011
- Thwaites, B. J., Reeve, P., Dinesh, N., Short, M. D., and van den Akker, B. (2017). “Comparison of an anaerobic feed and split anaerobic-aerobic feed on granular sludge development, performance and ecology,” *Chemosphere* 172, 408-417. DOI: 10.1016/j.chemosphere.2016.12.133
- Wan, C., Yang, X., Lee, D.-J., Liu, X., Sun, S., and Chen, C. (2014). “Partial nitrification of wastewaters with high NaCl concentrations by aerobic granules in continuous-flow reactor,” *Bioresource Technol.* 152, 1-6. DOI: 10.1016/j.biortech.2013.10.112
- Wang, Z., Gao, M., She, Z., Wang, S., Jin, C., Zhao, Y., Yang, S., and Guo, L. (2015). “Effects of salinity on performance, extracellular polymeric substances and microbial community of an aerobic granular sequencing batch reactor,” *Sep. Purif. Technol.* 144, 223-231. DOI: 10.1016/j.seppur.2015.02.042
- Welles, L., Lopez-Vazquez, C. M., Hooijmans, C. M., van Loosdrecht, M. C. M., and Brdjanovic, D. (2014). “Impact of salinity on the anaerobic metabolism of phosphate-accumulating organisms (PAO) and glycogen-accumulating organisms (GAO),” *Appl. Microbiol. Biotechnol.* 98(17), 7609-7622. DOI: 10.1007/s00253-014-5778-4
- Yang, Y.-C., Liu, X., Wan, C., Sun, S., and Lee, D.-J. (2014). “Accelerated aerobic granulation using alternating feed loadings: Alginate-like exopolysaccharides,” *Bioresource Technol.* 171, 360-366. DOI: 10.1016/j.biortech.2014.08.092
- Yu, C., Liu, X., Zhang, Q., He, X., Huai, W., Wang, B., Cao, Y., and Zhou, R. (2015). “Molecular genetic analysis of phosphomannomutase genes in *Triticum monococcum*,” *The Crop Journal* 3(1), 29-36. DOI: 10.1016/j.cj.2014.07.003

- Zahedipour, F., Dalirfardouei, R., Karimi, G., and Jamialahmadi, K. (2017). "Molecular mechanisms of anticancer effects of Glucosamine," *Biomed. Pharmacother.* 95, 1051-1058. DOI: 10.1016/j.biopha.2017.08.122
- Zengin, G. E., Artan, N., Orhon, D., Satoh, H., and Mino, T. (2011). "Effect of aspartate and glutamate on the fate of enhanced biological phosphorus removal process and microbial community structure," *Bioresource Technol.* 102(2), 894-903. DOI: 10.1016/j.biortech.2010.09.023
- Zielinski, N. A., Maharaj, R., Roychoudhury, S., Danganan, C. E., Hendrickson, W., and Chakrabarty, A. M. (1992). "Alginate synthesis in *Pseudomonas aeruginosa*: Environmental regulation of the algC promoter," *J. Bacteriol.* 174(23), 7680-7688. DOI: 10.1128/jb.174.23.7680-7688.1992

Article submitted: July 11, 2018; Peer review completed: September 17, 2018; Revised version received: November 10, 2018; Accepted: November 11, 2018; Published: November 14, 2018.

DOI: 10.15376/biores.14.1.139-166

SUPPLEMENTAL INFORMATION

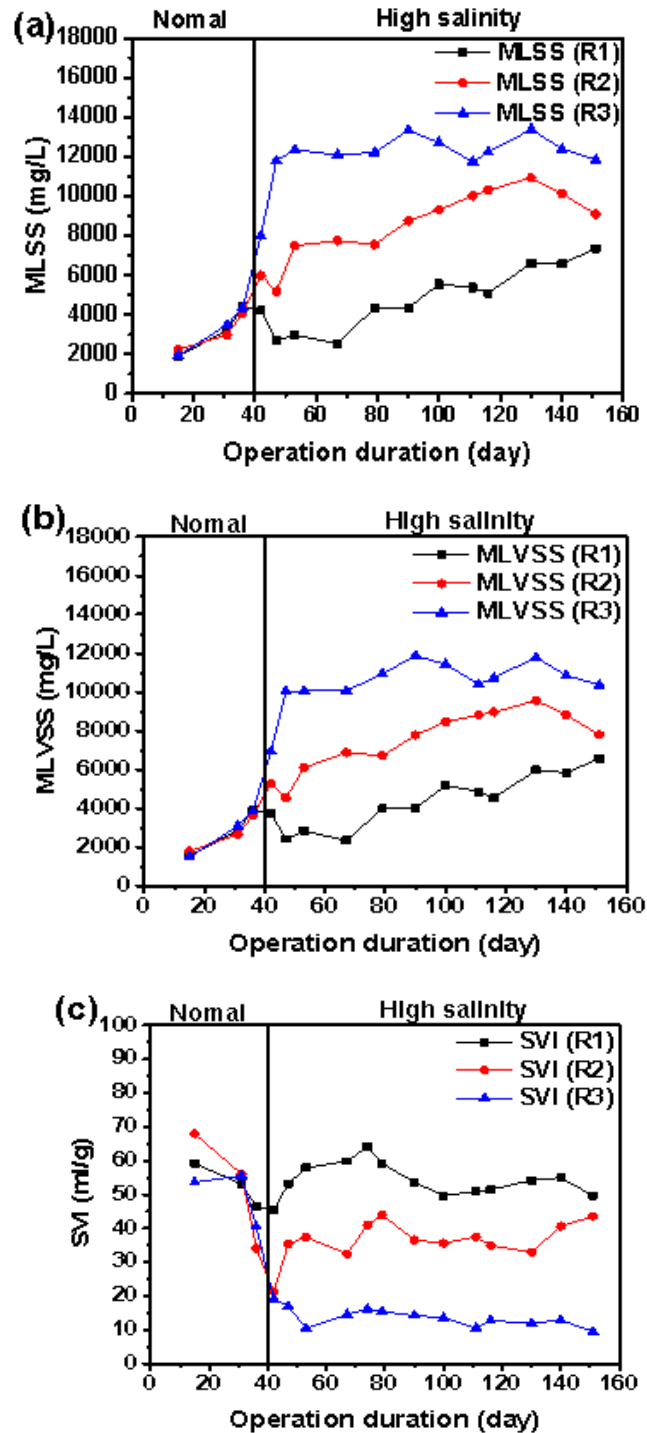


Fig. S1. Variation of MLSS (a), MLVSS (b) and SVI (30) during the cultivation

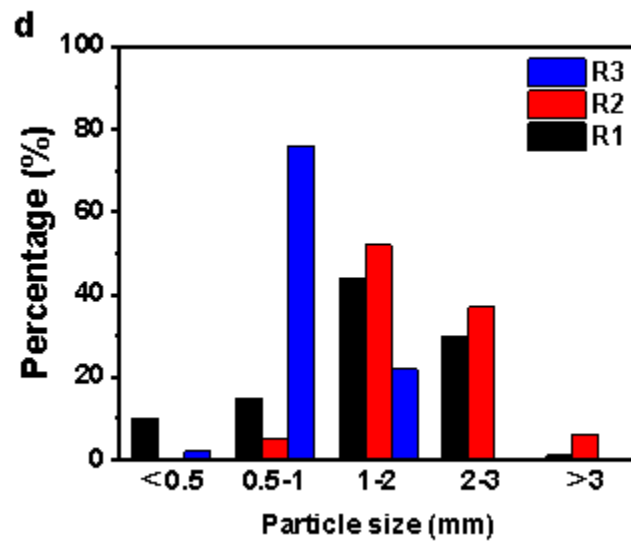
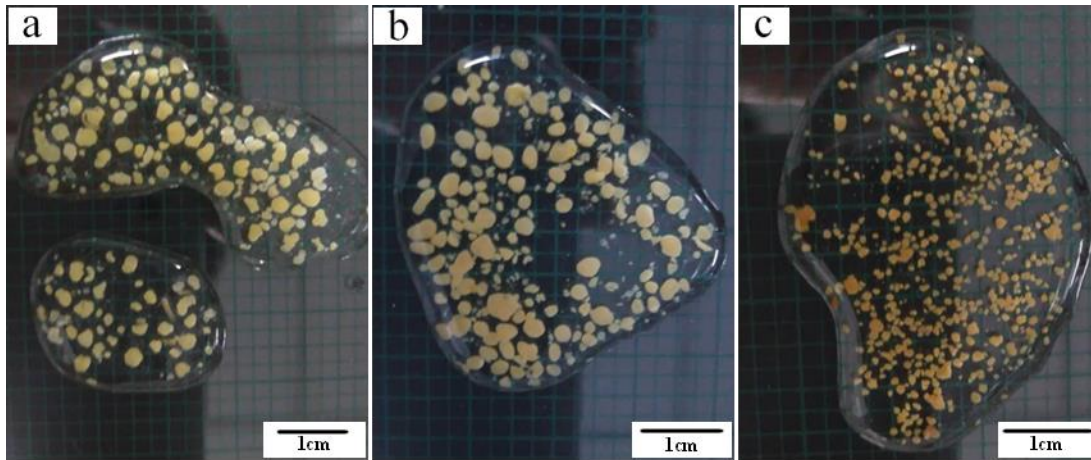


Fig. S2. Images of granular sludge from R1 (a), R2 (b), R3 (c) and granular particle size distribution (d) on 130 d

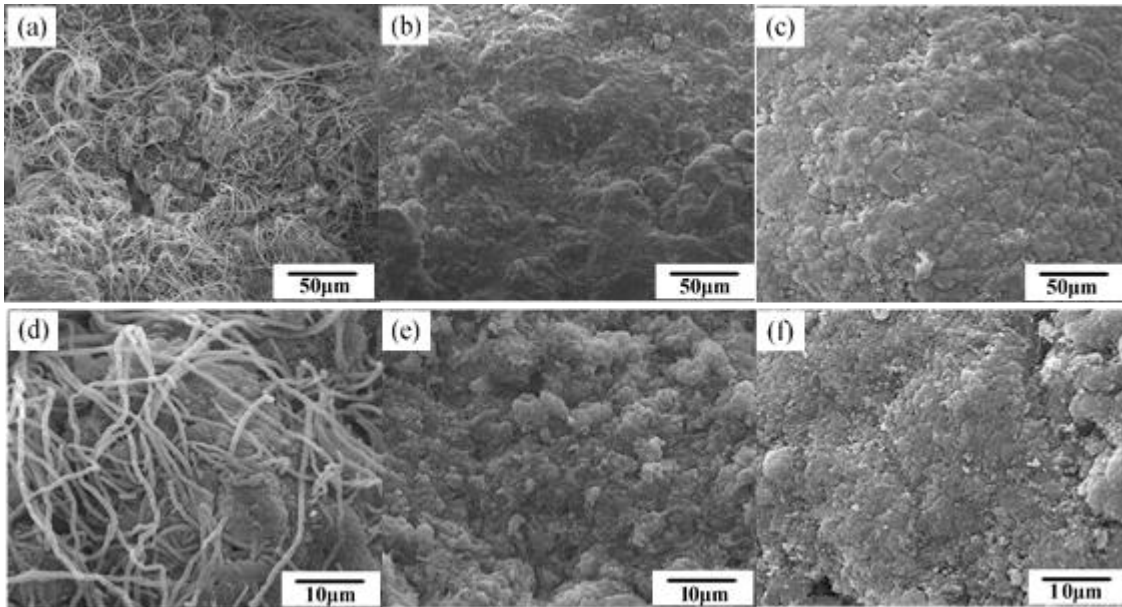


Fig. S3. SEM images of granular sludge from R1 (a, d), R2 (b, e) and R3 (c, f) on 130 d

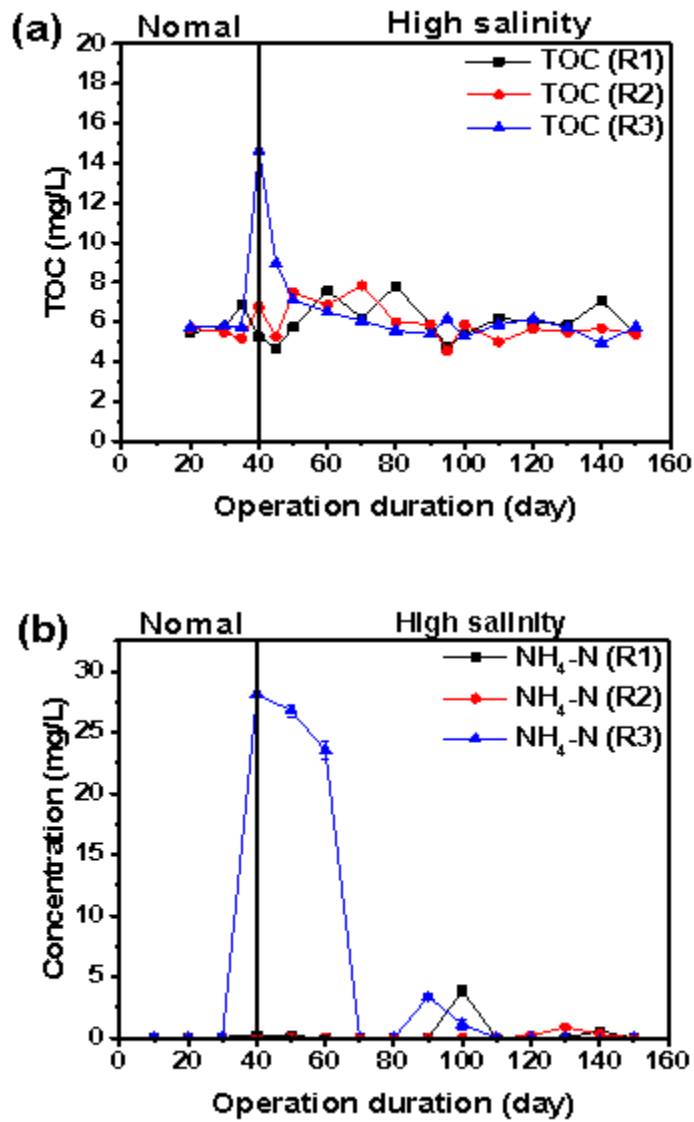


Fig. S4. Variation of TOC (a) and $\text{NH}_4\text{-N}$ (b) in the effluent during the cultivation

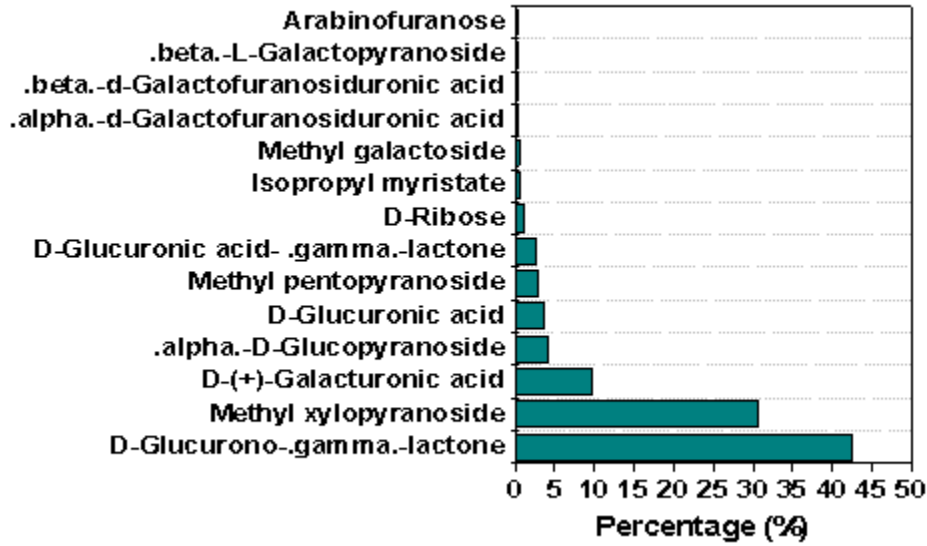


Fig. S5. GC-MS analysis for the standard alginate compositions

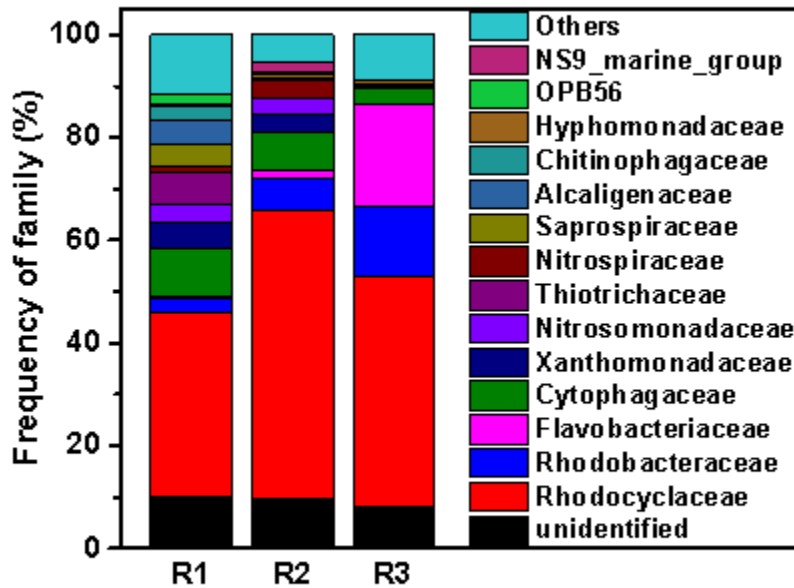


Fig. S6. Abundance of main families in the granules from R1, R2 and R3 on day 125

Table S1. Compounds Detected by GC-MS in the ALE of R1

No	RT	Compound name	Chemical formula	Mass	Similarity index	Percentage (%)
1	3.4	Glyceric acid, 3TMS derivative	C ₁₂ H ₃₀ O ₄ Si ₃	322.1	79.4	0.5%
2	4.2	Pyrimidine, 5-methyl-2,4-bis[(trimethylsilyl)oxy]-	C ₁₁ H ₂₂ N ₂ O ₂ Si ₂	270.1	89.4	1.7%
3	4.3	Methyl L-alaninate, 2TMS derivative	C ₁₀ H ₂₅ NO ₂ Si ₂	247.1	78.6	0.7%
4	4.8	Cytosine, trimethylsilyl ether	C ₇ H ₁₃ N ₃ OSi	183.1	79.4	1.0%
5	5.7	4-Pyrimidinamine, N-(trimethylsilyl)-2-[(trimethylsilyl)oxy]-	C ₁₀ H ₂₁ N ₃ OSi ₂	255.1	90.0	2.4%
6	6.2	Methyl .alpha.-D-ribofuranoside, 3TMS derivative	C ₁₅ H ₃₆ O ₅ Si ₃	380.2	84.0	0.7%
7	6.4	Xylopyranose, 3-O-methyl-1,2,4-tris-O-(trimethylsilyl)-	C ₁₅ H ₃₆ O ₅ Si ₃	380.2	75.1	0.2%
8	6.6	.beta.-L-Galactopyranoside, methyl 6-deoxy-, (S,S,R,R,S)-, 3TMS derivative	C ₁₆ H ₃₈ O ₅ Si ₃	394.2	94.2	15.0%
9	7.3	L-Rhamnose, 4TMS derivative	C ₁₈ H ₄₄ O ₅ Si ₄	452.2	96.4	4.6%
10	7.6	.alpha.-D-(-)-Ribopyranose, 4TMS derivative	C ₁₇ H ₄₂ O ₅ Si ₄	438.2	88.5	0.2%
11	7.6	Methyl xylopyranoside, 3TMS derivative	C ₁₅ H ₃₆ O ₅ Si ₃	380.2	93.5	5.2%
12	7.9	Methyl pentopyranoside, 3TMS derivative	C ₁₅ H ₃₆ O ₅ Si ₃	380.2	92.7	2.3%
13	8.4	D-Xylopyranose, 4TMS derivative	C ₁₇ H ₄₂ O ₅ Si ₄	438.2	94.6	1.4%
14	8.4	.beta.-L-(-)-Fucopyranose, 4TMS derivative	C ₁₈ H ₄₄ O ₅ Si ₄	452.2	86.4	1.0%
15	9.1	.beta.-D-(-)-Lyxopyranose, 4TMS derivative	C ₁₇ H ₄₂ O ₅ Si ₄	438.2	81.0	2.3%
16	9.3	Terephthalic acid, 2TMS derivative	C ₁₄ H ₂₂ O ₄ Si ₂	310.1	94.5	1.4%
17	9.4	Methyl galactoside (1S,2S,3S,4R,5R)-, 4TMS derivative	C ₁₉ H ₄₆ O ₆ Si ₄	482.2	95.1	7.4%
18	9.8	D-Mannose, 5TMS derivative	C ₂₁ H ₅₂ O ₆ Si ₅	540.3	93.5	1.7%
19	9.9	Methyl galactoside, 4TMS derivative	C ₁₉ H ₄₆ O ₆ Si ₄	482.2	86.1	2.6%
20	10	Methyl galactoside (1R,2R,3S,4S,5R)-, 4TMS derivative	C ₁₉ H ₄₆ O ₆ Si ₄	482.2	93.2	9.0%
21	10	D-(+)-Glucosamine, 4TMS derivative	C ₁₈ H ₄₅ NO ₅ Si ₄	467.2	86.9	5.6%
22	10.3	Adenine, 2TMS derivative	C ₁₁ H ₂₁ N ₅ Si ₂	279.1	84.4	2.1%
23	10.5	.beta.-D-(+)-Talopyranose, 5TMS derivative	C ₂₁ H ₅₂ O ₆ Si ₅	540.3	87.7	1.5%
24	10.5	.alpha.-D-Glucopyranoside, methyl 2,3,4-tris-O-(trimethylsilyl)-6-dodecanoyl-	C ₂₈ H ₆₀ O ₇ Si ₃	592.4	80.2	1.0%
25	10.8	Methyl galactoside (1S,2R,3S,4R,5R)-, 4TMS derivative	C ₁₉ H ₄₆ O ₆ Si ₄	482.2	94.8	6.5%
26	10.9	Glucopyranose, 5TMS derivative	C ₂₁ H ₅₂ O ₆ Si ₅	540.3	87.7	1.3%
27	11	D-(+)-Glucosamine, 6TMS derivative	C ₂₄ H ₆₁ NO ₅ Si ₆	611.3	83.9	5.3%
28	11.1	Talose, 5TMS derivative	C ₂₁ H ₅₂ O ₆ Si ₅	540.3	94.5	3.0%
29	11.2	Methyl galactoside, 3TMS derivative	C ₁₆ H ₃₈ O ₆ Si ₃	410.2	79.8	0.7%
30	11.5	D-(+)-Galacturonic acid, 5TMS derivative	C ₂₁ H ₅₀ O ₇ Si ₅	554.2	80.3	1.3%
31	12	D-Ribose, 4TMS derivative	C ₁₇ H ₄₂ O ₅ Si ₄	438.2	82.1	6.5%
32	12.5	Palmitic Acid, TMS derivative	C ₁₉ H ₄₀ O ₂ Si	328.3	79.1	0.1%
33	13.1	1,5-Anhydrohexitol, 4TMS derivative	C ₁₈ H ₄₄ O ₅ Si ₄	452.2	78.2	0.8%
34	13.6	D-Arabinopyranose, 4TMS derivative (isomer 1)	C ₁₇ H ₄₂ O ₅ Si ₄	438.2	77.1	0.5%
35	13.7	N,9-bis(Trimethylsilyl)-6-[(trimethylsilyl)oxy]-9H-purin-2-amine	C ₁₄ H ₂₉ N ₅ OSi ₃	367.2	93.2	2.3%
36	14.2	Methyl 14-methyl-3-(trimethylsilyloxy)hexadecanoate	C ₂₁ H ₄₄ O ₃ Si	372.3	82.0	0.1%

Table S2. Compounds Detected by GC-MS in the ALE of R2

No.	RT	Compound name	Chemical formula	Mass	Similarity index	Percentage (%)
1	4.2	Pyrimidine, 5-methyl-2,4-bis[(trimethylsilyl)oxy]-	C ₁₁ H ₂₂ N ₂ O ₂ Si ₂	270.1	87.4	1.5%
2	4.3	Methyl L-alaninate, 2TMS derivative	C ₁₀ H ₂₅ NO ₂ Si ₂	247.1	88.4	3.4%
3	4.8	Cytosine, trimethylsilyl ether	C ₇ H ₁₃ N ₃ O ₂ Si	183.1	81.0	0.6%
4	5.7	4-Pyrimidinamine, N-(trimethylsilyl)-2-[(trimethylsilyl)oxy]-	C ₁₀ H ₂₁ N ₃ O ₂ Si ₂	255.1	83.1	3.0%
5	6.2	Methyl .beta.-Arabinofuranoside, 3TMS derivative	C ₁₅ H ₃₆ O ₅ Si ₃	380.2	81.1	1.8%
6	6.4	Xylopyranose, 3-O-methyl-1,2,4-tris-O-(trimethylsilyl)-	C ₁₅ H ₃₆ O ₅ Si ₃	380.2	78.1	0.8%
7	6.6	.beta.-L-Galactopyranoside, methyl 6-deoxy-, (S,S,R,R,S)-, 3TMS derivative	C ₁₆ H ₃₈ O ₅ Si ₃	394.2	94.2	11.2%
8	7	.alpha.-L-Galactopyranoside, methyl 6-deoxy-, (R,R,R,S,S)-, 3TMS derivative	C ₁₆ H ₃₈ O ₅ Si ₃	394.2	78.2	1.0%
9	7.1	D-Ribose, 4TMS derivative	C ₁₇ H ₄₂ O ₅ Si ₄	438.2	85.1	1.4%
10	7.3	L-Rhamnose, 4TMS derivative	C ₁₈ H ₄₄ O ₅ Si ₄	452.2	96.4	4.1%
11	7.4	Octadecanamide, N-(2-methylpropyl)-N-nitroso-	C ₂₂ H ₄₄ N ₂ O ₂	368.3	77.9	4.2%
12	7.5	.alpha.-D-(-)-Ribopyranose, 4TMS derivative	C ₁₇ H ₄₂ O ₅ Si ₄	438.2	87.7	0.7%
13	7.6	Methyl xylopyranoside, 3TMS derivative	C ₁₅ H ₃₆ O ₅ Si ₃	380.2	84.3	1.0%
14	7.8	.beta.-D-(-)-Ribopyranose, 4TMS derivative	C ₁₇ H ₄₂ O ₅ Si ₄	438.2	77.0	0.3%
15	7.9	.alpha.-D-(-)-Lyxopyranose, 4TMS derivative	C ₁₇ H ₄₂ O ₅ Si ₄	438.2	86.9	0.5%
16	8.4	.beta.-L-(-)-Fucopyranose, 4TMS derivative	C ₁₈ H ₄₄ O ₅ Si ₄	452.2	76.2	1.5%
17	9.1	Phosphoric acid, bis(trimethylsilyl) 2,3-bis[(trimethylsilyl)oxy]propyl ester	C ₁₅ H ₄₁ O ₆ PSi ₄	460.2	90.2	2.8%
18	9.3	Terephthalic acid, 2TMS derivative	C ₁₄ H ₂₂ O ₄ Si ₂	310.1	90.2	1.6%
19	9.4	Methyl galactoside (1S,2S,3S,4R,5R)-, 4TMS derivative	C ₁₉ H ₄₆ O ₆ Si ₄	482.2	93.2	5.5%
20	9.8	.alpha.-D-Mannopyranose, 5TMS derivative	C ₂₁ H ₅₂ O ₆ Si ₅	540.3	89.2	1.3%
21	9.9	Methyl galactoside, 4TMS derivative	C ₁₉ H ₄₆ O ₆ Si ₄	482.2	83.8	2.5%
22	10	Methyl galactoside (1R,2R,3S,4S,5R)-, 4TMS derivative	C ₁₉ H ₄₆ O ₆ Si ₄	482.2	92.8	7.0%
23	10	D-(+)-Glucosamine, 4TMS derivative	C ₁₈ H ₄₅ NO ₅ Si ₄	467.2	85.2	11.1%
24	10.3	Adenine, 2TMS derivative	C ₁₁ H ₂₁ N ₅ Si ₂	279.1	85.2	2.1%
25	10.5	.beta.-D-(+)-Talopyranose, 5TMS derivative	C ₂₁ H ₅₂ O ₆ Si ₅	540.3	87.2	1.5%
26	10.5	Methyl galactoside, 3TMS derivative	C ₁₆ H ₃₈ O ₆ Si ₃	410.2	80.4	1.3%
27	10.8	Methyl galactoside (1S,2R,3S,4R,5R)-, 4TMS derivative	C ₁₉ H ₄₆ O ₆ Si ₄	482.2	95.3	9.7%
28	10.9	Glucopyranose, 5TMS derivative	C ₂₁ H ₅₂ O ₆ Si ₅	540.3	91.9	1.5%
29	11	D-(+)-Glucosamine, 6TMS derivative	C ₂₄ H ₆₁ NO ₅ Si ₆	611.3	89.1	6.0%
30	11.1	Talose, 5TMS derivative	C ₂₁ H ₅₂ O ₆ Si ₅	540.3	94.5	2.1%
31	12.1	.beta.-D-Glucopyranose, 5TMS derivative	C ₂₁ H ₅₂ O ₆ Si ₅	540.3	81.4	2.0%
32	12.4	1,5-Anhydrohexitol, 4TMS derivative	C ₁₈ H ₄₄ O ₅ Si ₄	452.2	76.9	1.8%
33	12.6	D-(+)-Galacturonic acid, 5TMS derivative	C ₂₁ H ₅₀ O ₇ Si ₅	554.2	77.9	0.1%
34	13.7	N,9-bis(trimethylsilyl)-6-[(trimethylsilyl)oxy]-9H-purin-2-amine	C ₁₄ H ₂₉ N ₅ O ₃ Si ₃	367.2	90.9	2.4%

35	14.2	Methyl 14-methyl-3-(trimethylsilyloxy)hexadecanoate	$C_{21}H_{44}O_3Si$	372.3	76.4	0.1%
36	16.1	.beta.-D-Galactopyranoside, methyl 2,3-bis-O-(trimethylsilyl)-, cyclic methylboronate	$C_{14}H_{31}BO_6Si_2$	362.2	77.2	0.1%
37	16.4	.alpha.-D-Glucopyranosiduronic acid, 3-(5-ethylhexahydro-2,4,6-trioxo-5-pyrimidinyl)-1,1-dimethylpropyl 2,3,4-tris-O-(trimethylsilyl)-, methyl ester	$C_{27}H_{52}N_2O_{10}Si_3$	648.3	75.5	0.2%
38	16.8	N-Acetyl glucosamine methoxime, tetrakis(trimethylsilyl)	$C_{21}H_{50}N_2O_6Si_4$	538.3	76.3	0.2%

Table S3. Compounds Detected by GC-MS in the ALE of R3

No.	RT	Compound name	Chemical formula	Mass	Similarity index	Percentage (%)
1	4.2	Pyrimidine, 5-methyl-2,4-bis[(trimethylsilyl)oxy]-	C ₁₁ H ₂₂ N ₂ O ₂ Si ₂	270.1	90.3	1.4%
2	4.3	Methyl L-alaninate, 2TMS derivative	C ₁₀ H ₂₅ NO ₂ Si ₂	247.1	76.5	0.6%
3	4.8	Cytosine, trimethylsilyl ether	C ₇ H ₁₃ N ₃ OSi	183.1	85.1	1.2%
4	5.7	4-Pyrimidinamine, N-(trimethylsilyl)-2-[(trimethylsilyl)oxy]-	C ₁₀ H ₂₁ N ₃ OSi ₂	255.1	89.0	2.1%
5	6.5	Methyl .alpha.-D-ribofuranoside, 3TMS derivative	C ₁₅ H ₃₆ O ₅ Si ₃	380.2	90.7	0.4%
6	6.6	.beta.-L-Galactopyranoside, methyl 6-deoxy-, (S,S,R,R,S)-, 3TMS derivative	C ₁₆ H ₃₈ O ₅ Si ₃	394.2	94.6	6.9%
7	6.8	2,6-Di-O-methyl-d-galactopyranose, 3TMS derivative	C ₁₇ H ₄₀ O ₆ Si ₃	424.2	75.8	0.4%
8	7.3	L-Rhamnose, 4TMS derivative	C ₁₈ H ₄₄ O ₅ Si ₄	452.2	95.4	2.5%
9	7.4	Octadecanamide, N-(2-methylpropyl)-N-nitroso-	C ₂₂ H ₄₄ N ₂ O ₂	368.3	75.4	0.6%
10	7.5	.alpha.-D-(-)-Ribopyranose, 4TMS derivative	C ₁₇ H ₄₂ O ₅ Si ₄	438.2	80.2	0.4%
11	8.3	.alpha.-L-Galactopyranoside, methyl 6-deoxy-, (R,R,R,S,S)-, 3TMS derivative	C ₁₆ H ₃₈ O ₅ Si ₃	394.2	78.0	0.3%
12	8.4	.beta.-L-(-)-Fucopyranose, 4TMS derivative	C ₁₈ H ₄₄ O ₅ Si ₄	452.2	81.6	2.0%
13	9.3	Terephthalic acid, 2TMS derivative	C ₁₄ H ₂₂ O ₄ Si ₂	310.1	95.1	1.7%
14	9.4	Methyl galactoside (1S,2S,3S,4R,5R)-, 4TMS derivative	C ₁₉ H ₄₆ O ₆ Si ₄	482.2	95.0	16.5%
15	9.8	D-Mannose, 5TMS derivative	C ₂₁ H ₅₂ O ₆ Si ₅	540.3	93.6	3.6%
16	9.9	Methyl galactoside, 4TMS derivative	C ₁₉ H ₄₆ O ₆ Si ₄	482.2	84.3	2.7%
17	10	D-(+)-Glucosamine, 4TMS derivative	C ₁₈ H ₄₅ NO ₅ Si ₄	467.2	83.1	5.6%
18	10.3	Adenine, 2TMS derivative	C ₁₁ H ₂₁ N ₅ Si ₂	279.1	85.9	1.9%
19	10.4	Methyl galactoside (1R,2R,3S,4S,5R)-, 4TMS derivative	C ₁₉ H ₄₆ O ₆ Si ₄	482.2	89.7	8.3%
20	10.5	Talose, 5TMS derivative	C ₂₁ H ₅₂ O ₆ Si ₅	540.3	91.9	8.9%
21	10.8	Methyl galactoside (1S,2R,3S,4R,5R)-, 4TMS derivative	C ₁₉ H ₄₆ O ₆ Si ₄	482.2	95.5	15.9%
22	11	D-(+)-Glucosamine, 6TMS derivative	C ₂₄ H ₆₁ NO ₅ Si ₆	611.3	84.5	1.9%
23	11.2	Methyl galactoside, 3TMS derivative	C ₁₆ H ₃₈ O ₆ Si ₃	410.2	80.1	3.8%
24	11.7	D-(+)-Galacturonic acid, 5TMS derivative	C ₂₁ H ₅₀ O ₇ Si ₅	554.2	86.6	2.2%
25	12.1	.beta.-D-Glucopyranose, 5TMS derivative	C ₂₁ H ₅₂ O ₆ Si ₅	540.3	85.3	3.1%
26	12.6	DL-Arabinopyranose, 4TMS derivative	C ₁₇ H ₄₂ O ₅ Si ₄	438.2	76.9	0.2%
27	13.1	1,5-Anhydrohexitol, 4TMS derivative	C ₁₈ H ₄₄ O ₅ Si ₄	452.2	77.7	1.2%
28	13.7	N,9-bis(Trimethylsilyl)-6-[(trimethylsilyl)oxy]-9H-purin-2-amine	C ₁₄ H ₂₉ N ₅ OSi ₃	367.2	91.3	2.2%
29	14.2	Methyl 14-methyl-3-(trimethylsilyloxy)hexadecanoate	C ₂₁ H ₄₄ O ₃ Si	372.3	87.6	0.4%
30	21.2	Maltose, 8TMS derivative, isomer 1	C ₃₆ H ₈₆ O ₁₁ Si ₈	918.4	81.8	0.6%
31	23.5	D-(+)-Cellobiose, (isomer 1), 8TMS derivative	C ₃₆ H ₈₆ O ₁₁ Si ₈	918.4	77.7	0.2%
32	23.8	L-(+)-Rhamnopyranose, 4TMS derivative	C ₁₈ H ₄₄ O ₅ Si ₄	452.2	81.3	0.2%